


ARTICLE

<https://doi.org/10.1038/s41467-019-09249-z>

OPEN

Axial shielding of Pd(II) complexes enables perfect stereoretention in Suzuki-Miyaura cross-coupling of Csp³ boronic acids

Jonathan W. Lehmann¹, Ian T. Crouch¹, Daniel J. Blair ¹, Melanie Trobe¹, Pulin Wang¹, Junqi Li¹ & Martin D. Burke^{1,2}

Stereocontrolled Csp³ cross-coupling can fundamentally change the types of chemical structures that can be mined for molecular functions. Although considerable progress in achieving the targeted chemical reactivity has been made, controlling stereochemistry in Csp³ cross-coupling remains challenging. Here we report that ligand-based axial shielding of Pd(II) complexes enables Suzuki-Miyaura cross-coupling of unactivated Csp³ boronic acids with perfect stereoretention. This approach leverages key differences in spatial orientation between competing pathways for stereoretentive and stereoinvertive transmetalation of Csp³ boronic acids to Pd(II). We show that axial shielding enables perfectly stereoretentive cross-coupling with a range of unactivated secondary Csp³ boronic acids, as well as the stereocontrolled synthesis of xylarinic acid B and all of its Csp³ stereoisomers. We expect these ligand design principles will broadly enable the continued search for practical and effective methods for stereospecific Csp³ cross-coupling.

¹Department of Chemistry, University of Illinois at Urbana-Champaign, 454 Roger Adams Laboratory, 600S Mathews Avenue, Urbana 61801 IL, USA. ²Carle Illinois College of Medicine, Institute for Genomic Biology, Beckman Institute, and Department of Biochemistry, University of Illinois at Urbana-Champaign, Urbana 61801 IL, USA. These authors contributed equally: Jonathan W. Lehmann, Ian T. Crouch. Correspondence and requests for materials should be addressed to M.D.B. (email: mdburke@illinois.edu)

The synthesis of stereochemically complex Csp³-rich small molecules remains a rate-limiting factor in the discovery and development of next generation medicines, agrochemicals, biological probes, materials, and many other types of societally impactful compounds^{1,2}. Suzuki-Miyaura cross-coupling has profoundly enabled progress with Csp²-rich molecules in all of these areas. Expanding this methodology to include stereocontrolled Csp³ cross-coupling could fundamentally change the types of molecular solutions that can be practically developed¹⁻³.

Stereochemical control in Csp³ cross-coupling can be pursued via either stereoselective or stereospecific pathways⁴. In stereoselective Csp³ cross-coupling, stereocontrol typically relies on subtle interactions between chiral catalysts and chiral substrates in stereoconvergent processes^{2,4}. Stereoselectivities thus tend to vary based on the structures of the cross-coupling partners employed (Fig. 1a, left)²⁻⁴. In contrast, stereospecific Csp³ coupling has the theoretical potential to employ achiral catalysts that perfectly translate into targeted products the stereochemistry that has been pre-installed into configurationally stable building blocks (Fig. 1a, right)³⁻⁶. Achieving this goal with generally non-toxic Csp³ boronic acids or their derivatives is particularly attractive^{1-4,7-9}. In a landmark paper¹⁰, Cruden and coworkers

first demonstrated in 2009 that configurationally stable, chiral non-racemic benzylic pinacol boronic esters can be cross-coupled with retention of stereochemistry, opening the door to this approach.

There is a fundamental challenge, however, that can make it difficult to achieve perfect stereocontrol in such reactions. There are two different stereospecific pathways for transmetalation of Csp³ boronic acids to Pd(II), and these two pathways are stereodivergent; one leads to inversion and the other leads to retention of configuration at the Csp³ carbon that is being transferred (Fig. 1b)^{3,11,12}. Consequently, the stereo-outcome for cross-couplings of even perfectly stereodefined Csp³ boronates can vary widely, or even reverse, depending on the substrate and/or reaction conditions^{3,4,10-19}. A number of reports have shown that competition between these two pathways can be at least partially controlled via specifically positioned activating groups in the Csp³ boronate substrates^{3,10-16,18}. A potential advantage of the existence of the two competing stereochemical courses is that a single enantioenriched substrate can provide both enantiomers of coupling products by careful tuning of reaction conditions³. This was first demonstrated by Suginome and coworkers using externally added Lewis acids to control the reversible intramolecular ligation between pinacol boronic esters and proximal Lewis

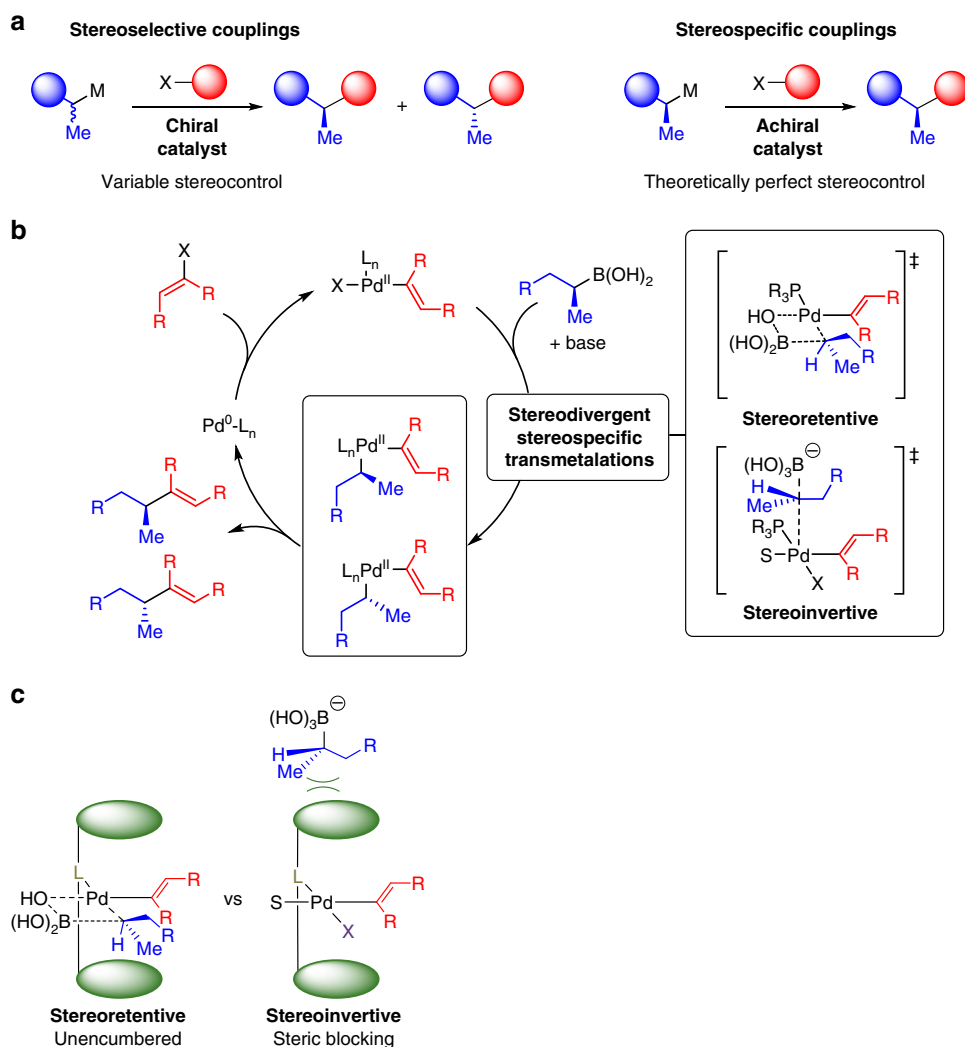


Fig. 1 Challenges in stereocontrolled Csp³ couplings. **a** Stereoselective couplings vs. stereospecific couplings. **b** Competing stereodivergent stereospecific transmetalation pathways. **c** Axial shielding—a ligand design principle for controlling stereochemistry in Csp³ couplings. Projecting steric bulk above and below the Pd (II) square plane should selectively inhibit stereoinvertive transmetalation, thus favoring stereoretention

basic amides¹¹. However, with all of these approaches, variable levels of stereocontrol is observed depending on the structures of the cross-coupling partners employed, which can lead to challenging-to-separate mixtures of stereoisomeric products. In order to access the still largely untapped potential for stereospecific cross-coupling of Csp^3 boronates to enable modular synthesis of complex Csp^3 -rich targets, approaches for rationally differentiating between the stereodivergent pathways for transmetalation to Pd(II) are needed. Herein we report that ligand-mediated axial shielding of a square planar Pd(II) complex enables Suzuki-Miyaura cross-couplings of a wide range of unactivated Csp^3 boronic acids to proceed with perfect stereoretention.

Results

Axial shielding to promote stereoretentive Csp^3 couplings.

Multiple lines of evidence support a model in which transmetalation of Csp^3 boronic acids can proceed through the two stereodivergent pathways depicted in Fig. 1b^{3,8,9}. Stereoretentive transmetalations likely involves a closed, four-membered transition state within the Pd(II) square plane³. This is similar to the transmetalation pathway that has recently been characterized for Csp^2 boronic acids^{20–23}. In that case, kinetic studies suggested that coordination of the boronic acid with a palladium hydroxo complex precedes transmetalation^{20,21}, and rapid injection, low-temperature NMR studies have recently characterized such intermediates^{22,24}. Computational studies have further shown that the transition state in which the nascent Pd–C bond is *trans* to the phosphine ligand is nearly 10 kcal/mol lower in energy relative to the *cis* counterpart due to less steric crowding²⁴. Related inner-sphere transmetalations with other Csp^3 organometallic coupling partners proceed with retention of stereochemistry^{25–27}. Alternatively, the transition state for stereoinvertive transmetalation likely involves backside electrophilic attack by Pd(II) on the boron-bearing carbon of an anionic trihydroxyborate^{3,11,12}. Ligand substitution reactions on 16-electron d8 square planar complexes usually proceed through associative mechanisms which involve 18-electron complexes and ligand approach at the axial positions above or below the metal square plane^{26,28}. Related stereoinvertive transmetalations of alkylstannanes similarly occur through an associative mechanism involving approach of the alkylstannanes orthogonal to the Pd(II) square plane²⁶.

Spatial differences between these stereodivergent transmetalation pathways suggested an opportunity to rationally discriminate between them via ligand-based axial shielding. Specifically, we reasoned that ligands which preferentially shield the axial positions by projecting steric bulk above and below the Pd(II) square plane should selectively block stereoinvertive transmetalation, thus favoring stereoretention (Fig. 1c). Encouraging precedent for this concept can be found in Brookhart's classic studies on the rates of associative addition of ethylene to Pd(II) complexes with variably shielded axial sites and the corresponding impacts on ethylene polymerization^{29,30}.

With this axial shielding design principle in mind, we were intrigued by the X-ray crystal structure of the oxidative addition adduct $\{[(2-Me-Ph)_3P]Pd(4-nBu-Ph)(Br)\}_2$ (Fig. 2a)³¹. We noted that in this Pd(II) complex, one *ortho*-methyl group projects above and another projects below the Pd(II) square plane. The resulting zig-zag-like orientation of these methyl groups is represented schematically below the crystal structure. This analysis suggests that axial shielding by these *ortho*-methyl groups will disfavor the invertive transmetalation pathway. As a result, relative to triphenyl phosphine, tri-*ortho*-tolyl phosphine would be expected to show increased stereoretention in cross-coupling of Csp^3 boronates. We reasoned that further increasing

steric bulk at the *ortho*-positions should increasingly block the stereoinvertive pathway via enhanced axial shielding while leaving the Pd(II) square plane unencumbered, thus leading to highly stereoretentive Csp^3 cross-couplings. $P(o-tol)_3$ has also been shown to disfavor β -hydride elimination³², which is an important additional advantage for Csp^3 coupling (vide infra).

We thus tested how different *ortho*-substituted triarylphosphine ligands impact the enantiospecificity of a representative cross-coupling of an unactivated chiral Csp^3 boronic acid (**S**)-**1a** with *para*-bromobiphenyl **2a**. (Fig. 2b). We began our studies with $Pd(PPh_3)_4$ as the catalyst and Ag_2O as base, as originally reported by Crudden and coworkers in the stereospecific cross-coupling of benzylic pinacol esters^{10–13}. A survey of alternative bases and solvents demonstrated that Ag_2O and dioxane were optimal. A reduced yield was observed with Ag_2CO_3 , and non-silver-containing bases provided no yield (Supplementary Figure 1a)^{33,34}. Attempts to couple the Bpin derivative of **1a** yielded none of the cross-coupling product. Using (**S**)-**1a** as the substrate and $Pd(PPh_3)_4$ as catalyst, we observed the stereoretentive product (+)-**3a**, but with only 21% enantiospecificity (Fig. 2b, entry 1). Replacing triphenylphosphine with $P(o-tol)_3$ (entry 2) increased the enantiospecificity to 86%. Further increasing the size of the *ortho* substituents to ethyl groups (entry 3) increased the enantiospecificity to 91%. Finally, near perfect enantiospecificity (98%) was achieved with the ligand, tri(2-benzyl-phenyl)phosphine, **L4** (entry 4). Notably, across the same series of ligands, the yield and branched/linear (*b/l*) ratios also increased in parallel, such that **L4** provided a yield of 72% and a near-perfect *b/l* ratio (>250/1). Alternatively performing this reaction with 1 equiv. of boronic acid **1a** and 2 equiv. of halide **2a** provided a 30% yield based on the limiting boronic acid (Supplementary Figure 1b).

To gain insight into how **L4** promotes such high levels of stereoretention, we obtained a crystal structure of the dimeric Pd(II) oxidative addition adduct $\{[(2-Bn-Ph)_3P]Pd(4-OMe-Ph)(Br)\}_2$ (Fig. 2c). Like the corresponding $P(o-tol)_3$ complex (Fig. 2a), one of the benzyl groups is rotated to project away from the Pd center, and the remaining two sterically bulky benzyl substituents are projected above and below the square plane of the Pd(II) complex. These results are consistent with the model in which increased axial shielding selectively inhibits a competing stereoinvertive transmetalation pathway (Fig. 1c).

We also considered the alternative possibility that the improved enantiospecificity for ligands **L1–L4** was attributable to mitigation of a potential alternative pathway for racemization involving β -hydride elimination followed by hydropalladation of a prochiral olefin (Supplementary Figure 2)³. In this scenario, the enantiospecificity would be expected to increase in parallel with the *b/l* ratio, as we observed for **L1–L4**. However, three distinct lines of evidence suggest that the enantiospecificities and *b/l* ratios are not mechanistically coupled.

First, we also prepared a tri-*ortho*-cyclohexyl phenyl phosphine ligand, **L5**, which may be too large and therefore sterically encumber the Pd(II) square plane. This ligand provided the product (+)-**3a** with a nearly identical *b/l* ratio but substantially reduced enantiospecificity relative to the same reaction performed under otherwise identical conditions with **L2** (Fig. 2d). Second, we synthesized a series of derivatives of $P(o-tol)_3$ with 1,2, or 3 deuterium atoms incorporated into each of the *ortho*-methyl groups (**L6–L8**). Such deuteration would not be expected to significantly modify the extent of axial shielding, but may impact the rate of β -hydride elimination³⁵. We observed no increase in enantiospecificity but progressive increases in *b/l* ratios with increasing levels of deuteration (Fig. 2d). Third, as detailed below, we observed anti-correlations between enantiospecificity and *b/l* ratios when **L2** was electronically tuned (Fig. 3a, b).

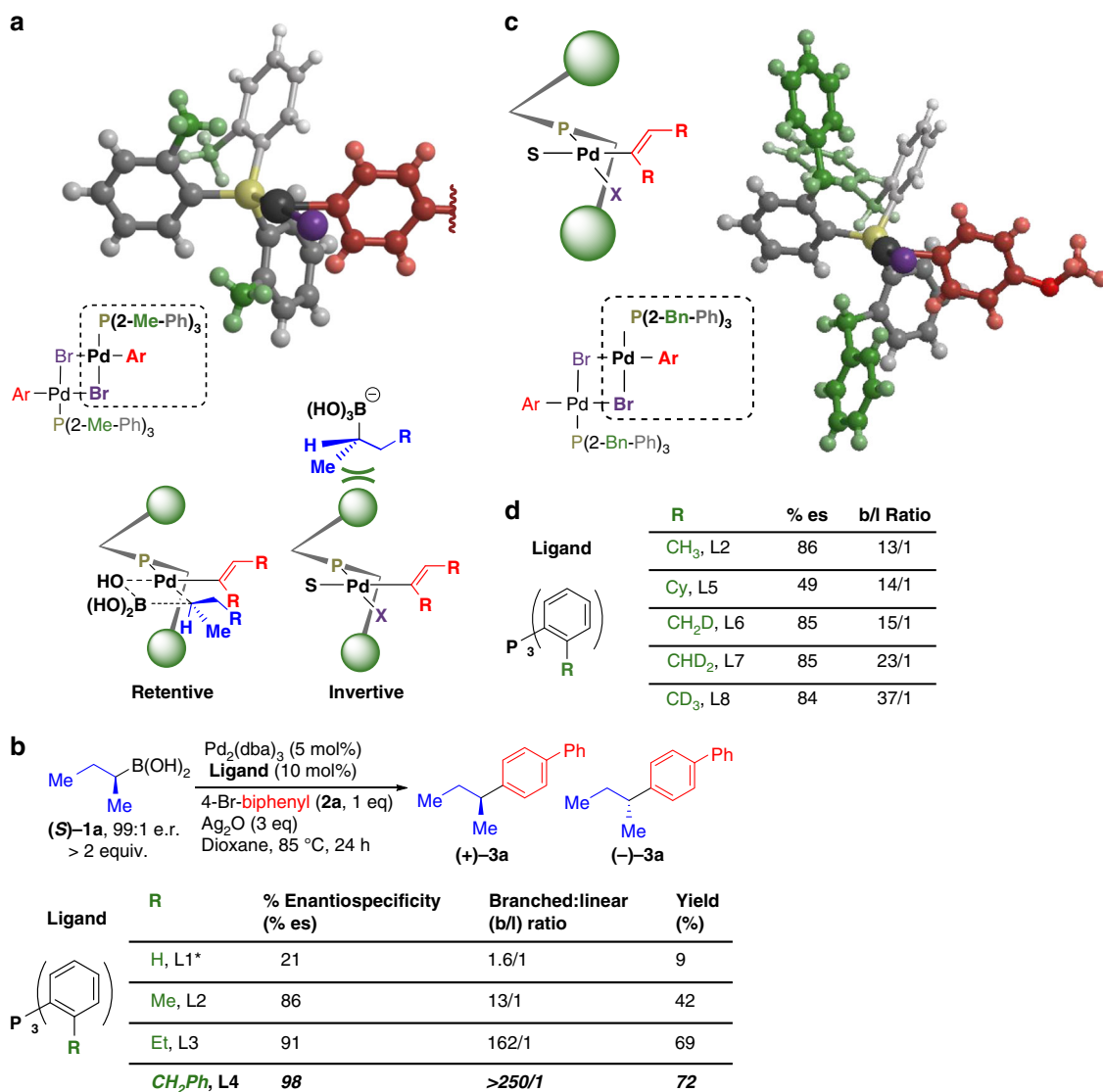


Fig. 2 Tuning of ligand sterics. **a** Crystal structure of $\{[(2\text{-Me-Ph})_3\text{P}]\text{Pd}(4\text{-}n\text{Bu-Ph})(\text{Br})\}_2$ and concept of blocking of the axial sites on Pd. **b** Model coupling reaction for optimizing ligands (*ortho*-substituent optimization) Pd(PPh₃)₄ was used due to insufficient yield with Pd₂dba₃/PPh₃. **c** Crystal structure of $\{[(2\text{-Bn-Ph})_3\text{P}]\text{Pd}(4\text{-OMe-Ph})(\text{Br})\}_2$ is consistent with the axial shielding ligand design principle. **d** % es and *b/l* ratio do not necessarily correlate as a function of ligand structure

Combining axial shielding with ligand electronic effects. During the course of our studies, we also observed interesting effects on both stereoselectivity and *b/l* ratios when we combined the axial shielding approach with electronic tuning of the ligands. We were initially intrigued by our observations of stereodivergence when we cross-coupled (S)-1a or its trifluoroborate counterpart ((S)-1a') under identical conditions, including both aqueous basic conditions as well as anhydrous conditions (Fig. 3a, b). As recently shown, P(*t*Bu)₃ promotes the primarily stereoinvertive Csp³ cross-coupling of 2-butyl potassium trifluoroborate (S)-1a' with aryl chloride 2a¹⁶, whereas we found that P(*o*-tol)₃ L2 leads primarily to stereoretention under these coupling conditions. We noted that these two ligands have similar cone angles [P(*t*Bu)₃, cone angle $\theta = 182^\circ$; L2, $\theta = 194^\circ$]³⁶ but different Tolman Parameters [P(*t*Bu)₃, $\nu = 2056.1\text{ cm}^{-1}$; L2, $\nu = 2066.6\text{ cm}^{-1}$]³⁶. We thus questioned whether ligand electronics might provide a second handle to further fine tune stereochemical control in combination with axial shielding.

We therefore synthesized and tested (Supplementary Figure 3) a systematically varied series of P(*o*-tol)₃ derivatives L10-L19

with a range of electron-donating and electron-withdrawing functional groups at the position *para* to the phosphorus atom (Fig. 3a, b). Such modifications represent more fine-tuning of the electronic nature of the phosphine ligands (Tolman Parameters for P(4-R-Ph)₃: R = OMe, $\nu = 2066.1\text{ cm}^{-1}$; R = H, $\nu = 2068.9\text{ cm}^{-1}$; R = F, $\nu = 2071.3\text{ cm}^{-1}$)³⁶. Under both sets of cross-coupling conditions, we observed a strong positive correlation ($R^2 = 0.97$ and 0.84) between the electron-deficient nature of the phosphine ligand and the enantiospecificity of the coupling reaction under both aqueous and anhydrous conditions (Fig. 3a, b). While this paper was under review, similar electronic trends were reported by Biscoe and Sigman³⁷.

We also observed generally decreased *b/l* ratios as ligands became more electron-deficient (Fig. 3a, b, Supplementary Figure 3). As noted above, this provides a third line of evidence that enantiospecificity and *b/l* ratios are not necessarily linked via a common mechanism. The more electron-deficient ligands also tended to provide lower yields. Moreover, even with the most electron-deficient variants of L2, the levels of stereoretention were inferior to those observed with the more axially shielding ligand P(2-Bn-Ph)₃ L4.

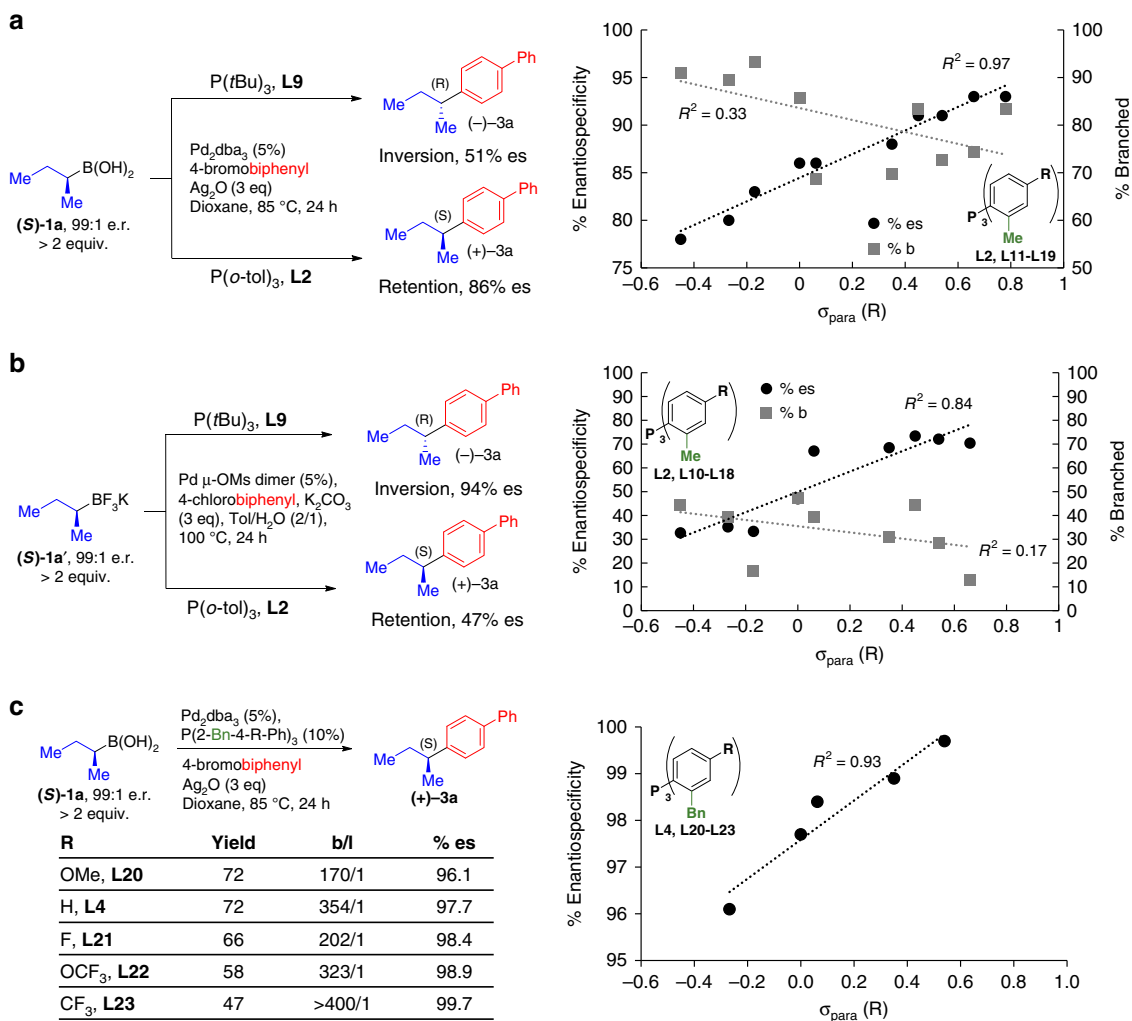


Fig. 3 Tuning of ligand electronics. The effect of ligand electronic tuning on stereooutcome and *b/l* ratio under both anhydrous (**a**) and biphasic (**b**) conditions (%branched = %b-%). **c** Electronic tuning of **L4** leads to perfect enantiospecificity for the cross-coupling of challenging substrate (**S-1a**)

We thus also synthesized a similar series of electronically tuned variants of **L4**. We again observed a strong positive correlation ($R^2 = 0.93$) between electron deficiency and enantiospecificity, with the most electron-poor derivative P(2-Bn-4-CF₃-Ph)₃ **L23** yielding perfect stereoretention (>99%), albeit with reduced yield (Fig. 3c).

Collectively, these results show that axial shielding can be combined with electronic tuning to maximize stereoretention in the cross-coupling of a very small and thus especially challenging Csp³ boronic acid such as (**S-1a**). However, given the corresponding reductions in yield and/or *b/l* ratios, we questioned whether more sterically bulky Csp³ boronic acids, which should be more sensitive to steric effects, might be coupled with near perfect stereoretention using only the axial shielding approach.

Axial shielding yields perfect stereoretention. Exploring the reaction scope for cross-coupling with axially shielding ligand **L4** first required access to a series of unactivated chiral non-racemic boronic acids in highly enantiomerically enriched form. Chiral derivatives of *N*-methyliminodiacetic acid (MIDA) have previously been used to promote diastereoselective epoxidations³⁸ and resolution of atropdiastereomeric biaryl boronic acids³⁹. We found that upon complexing a range of racemic secondary alkylboronic acids with a homochiral MIDA variant,

N-2-benzyloxycyclopentyl-iminodiacetic acid (BIDA), the diastereomeric BIDA boronates could be readily separated by chromatography and/or recrystallization to provide highly enantioenriched boronic acids (≥99:1 enantiomeric ratio (e.r.)) masked as air-stable building blocks (Supplementary Figure 4).

We found that best results in the subsequent Csp³ coupling reactions were achieved using anhydrous solutions of pure boronic acids. To prepare such solutions without forming boroxines, we hydrolyzed the BIDA boronates, added sodium hydroxide to generate the corresponding sodium trihydroxyborate salts⁴⁰, collected them by filtration and then treated these salts with one equivalent of BF₃•OEt₂ to generate anhydrous solutions of the free boronic acids (Fig. 4a).

Using this methodology, a range of unactivated secondary Csp³ boronic acids (**1a–1d**) were prepared in ≥99:1 e.r. (Supplementary Figure 4) and tested in cross-coupling reactions promoted by **L4** (Fig. 4b). In general, the boronic acids are fully consumed in these reactions. Perfect stereoretention was observed in most cases. A trifluoromethyl group (**3b**), a benzyl ether (**3c**) and beta branching (**3d**) were compatible with this reaction. All of these boronic acids also coupled in good yields and with *b/l* ratios > 250/1 (**1a–1d**). Moving the boronic acid to a more internal position along a linear alkyl chain was somewhat tolerated (**3e** and **3g**), but not beyond 2 carbon atoms (**3f**). For 3-hexylboronic acid (**1g**), a unique example of cross-coupling an

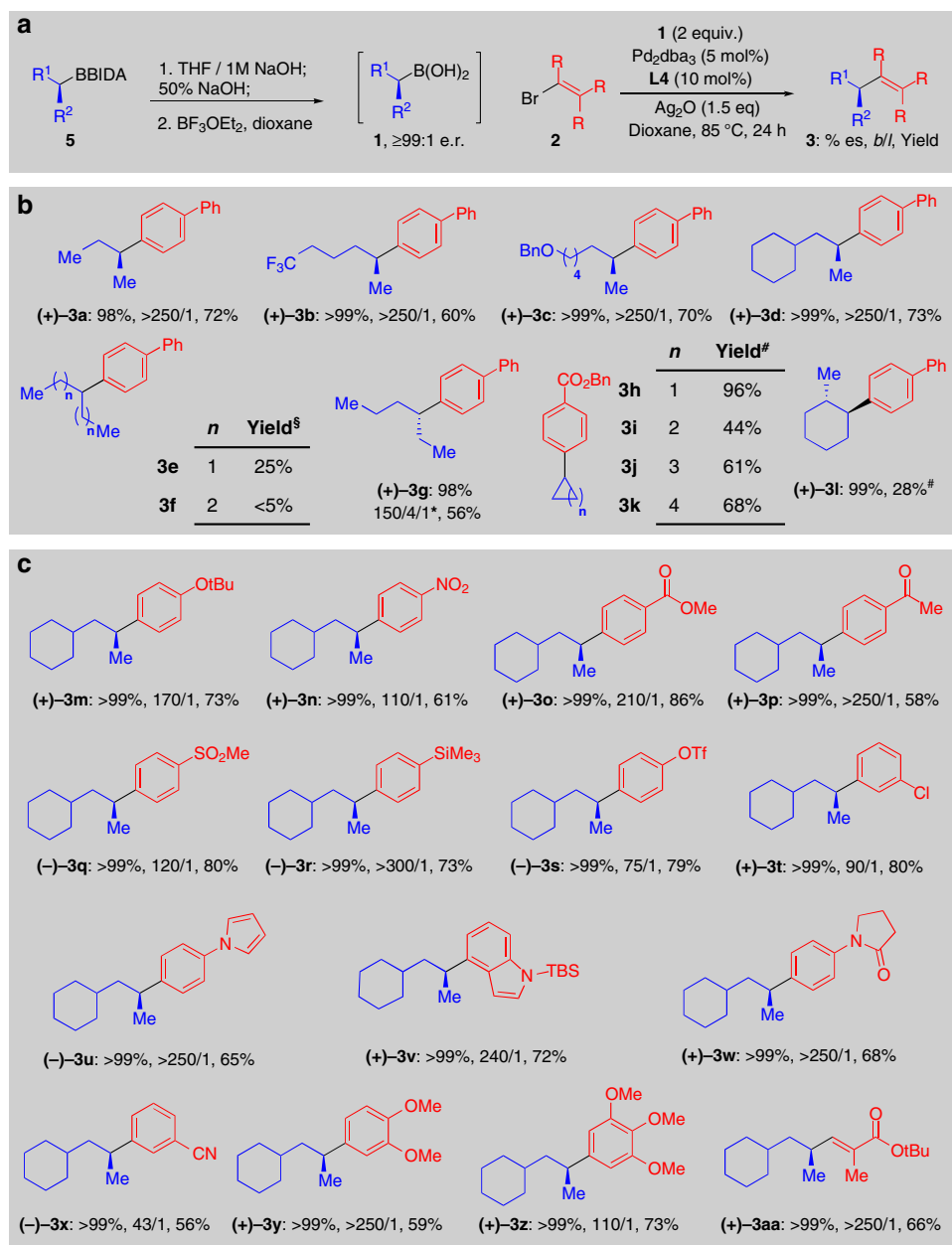


Fig. 4 Substrate scope of the stereospecific cross-coupling reaction. **a** Reaction conditions. **b** Scope of the Csp³ boronic acid coupling partner, ([§]: no improvement when using **L2**, [†]: branched on C3/branched on C2/linear (Supplementary Figure 5), [#]: **L2** was used, **L4** gave lower yields). **c** Scope of the bromide coupling partner. All reactions were performed in duplicate. Branched/linear ratios were determined by HPLC or GC analysis of the crude reaction using an authentic linear product standard. Yields were determined by isolation. Enantiospecificities were determined by chiral HPLC of the purified product

unactivated ethyl-branched chiral Csp³ boronic acid, we observed a 150/4/1 product distribution of the desired 3-hexyl (**3g**) to 2-hexyl (**3g'**) to 1-hexyl isomers (**4g**) and near perfect stereoretention (Supplementary Figure 5). A range of cyclic boronic acids (**3h–k**) were also effective using **L2** rather than **L4**. We also prepared and cross-coupled non-racemic 2-methyl cyclohexyl boronic acid (**11**), and observed perfect diastereo- and enantiospecificity (**3l**). The latter result shows that the Pd catalyst does not walk around the ring via sequential cycles of β -hydride elimination and hydropalladation to yield the enantiomeric product (Supplementary Figure 6).

Perfect stereoretention was also observed for cross-coupling with a wide range of electron-rich and electron-poor aryl halides (Fig. 4c). The functional group tolerance of this method was also found to include ethers (**3m**, **3y**, **3z**), nitro groups (**3n**), esters

(**3o**), ketones (**3p**), sulfones (**3q**), silanes (**3r**), and nitriles (**3x**). Although aryl triflates and aryl chlorides were poor coupling partners, their lack of reactivity provided the opportunity for halide-selective coupling (**3s**, **3t**). Some heterocycles, including pyrroles (**3u**) and indoles (**3v**), were also well-tolerated. Finally, we observed a cross-coupling in which perfect stereoretention is observed at both the Csp³ and Csp² centers between an unactivated secondary boronic acid and an activated vinyl halide (**3aa**).

Perfectly stereocontrolled synthesis of Csp³-rich molecules. We finally tested the capacity of this method to enable stereocontrolled Lego-like assembly⁹ of Csp³-rich natural products. One of the key strengths of this approach is the theoretical

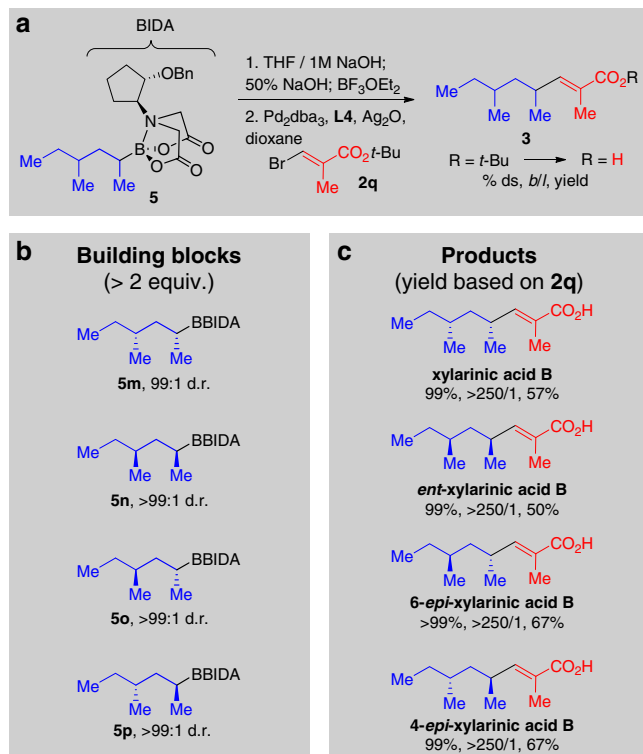


Fig. 5 Building block-based synthesis of all possible Csp³ stereoisomers of xyloaric acid B. **a** Conditions for deprotection and coupling. **b** Air-stable BIDA boronate building blocks prepared by resolution. **c** Xyloaric acid B and all possible Csp³ stereoisomers accessed by stereospecific cross-coupling of stereodefined building blocks. % ds, b/l, and yield refer to the cross-coupling step

potential to access all possible Csp³ stereoisomers with perfect stereocontrol by employing the corresponding series of pre-fabricated, stereochemically defined chiral building blocks. The recently discovered antifungal natural product xyloaric acid B^{41,42} served as an excellent case study (Fig. 5).

Leveraging the simple BIDA boronate resolution method, all of the required secondary Csp³ boronate building blocks were prepared in ≥99:1 diastereomeric ratio (d.r.) (Fig. 5b). All four of these building blocks proved to be air- and chromatographically stable crystalline solids.

This set the stage for the simple modular assembly of xyloaric acid B, and all of its Csp³ stereoisomers, via cross-coupling of these four stereodefined building blocks. Each building block was deprotected to the corresponding boronic acid, stereospecifically cross-coupled to vinyl bromide 2q using axially shielding ligand L4, and then deprotected under standard conditions (TFA/DCM). Through this simple approach, xyloaric acid B and all three of its Csp³ stereoisomers were readily accessed in perfect diastereospecificity (≥99%), >250/1 b/l ratios, and ≥50% yield (Fig. 5c).

We have found that axial shielding of Pd(II) complexes can lead to perfect stereoretention in the Suzuki–Miyaura cross-coupling of unactivated Csp³ boronic acids. Optimizations can also be achieved with especially challenging substrates by combining axial shielding with ligand electronic tuning. A wide range of phosphine ligands may be good candidates for similar steric and/or electronic tuning to rationally promote stereocontrolled Csp³ coupling. These principles might also be extended to the stereospecific coupling of other types of configurationally stable coupling partners, such as alkylstannanes and alkylsilanes, which have also been proposed to proceed via energetically

competitive stereodivergent transmetalation pathways with open and closed transition states^{27,43,44}. Continued progress in such directions stands to help enable the transformative potential impact of stereocontrolled Csp³ cross-coupling to be realized.

Methods

Synthesis of MIDA and BIDA boronates. To a 250-mL round-bottom flask with a stir bar was added racemic boronic acid (10 mmol, 1.0 equiv.), N-methylimidodiacetic acid (MIDA) (1.77 g, 12 mmol, 1.2 equiv.) and DMSO (10 mL, 1.0 M in boronic acid), and toluene (90 mL, 0.11 M in boronic acid). The mixture was fitted with a Dean Stark trap, on top of which was fitted a reflux condenser. The mixture was heated to reflux and water was collected in the trap for 2 h, at which point complete conversion of the boronic acid was confirmed by TLC. The toluene was then removed by rotary evaporation, H₂O (75 mL) was added, and the mixture was extracted with EtOAc (5 × 75 mL). The combined organic layers were washed with H₂O (5 × 75 mL). The organic phase was then dried over Na₂SO₄ and concentrated under vacuum to give the corresponding MIDA boronate as a white solid which was used without purification. The synthesis of BIDA boronates was performed with this same procedure, using 2,2'-((1*S*,2*S*)-2-(benzyloxy)cyclopentyl)azanediyl) diacetic acid (BIDA) (2.55 g, 8.3 mmol, 0.83 equiv.) instead of MIDA. The resulting diastereomeric mixtures were resolved by recrystallization from acetone and/or column chromatography and then used directly for the synthesis of sodium alkyltrihydroxyborate salts. For full experimental details, ¹H NMR, and ¹³C NMR spectra see Supplementary Methods.

Synthesis of sodium alkyltrihydroxyborate salts. To a stir bar-equipped 250-mL round-bottom flask under air was added MIDA or BIDA boronate (6.499 mmol, 1.00 equiv.), THF (33 mL, 0.20 M) and freshly prepared aqueous NaOH (1 M, 33 mL, 5.0 equiv.). The mixture was stirred at 23 °C until complete conversion was confirmed by TLC. THF was removed under rotary evaporation (bath temperature 40 °C). When most of the THF was removed, the receiving flask was emptied, dried and rotary evaporation was then continued until water began to collect in the receiving flask indicating complete removal of THF. Saturated NH₄Cl (33 mL) was added to the resulting aqueous solution and the aqueous layer was extracted with MTBE (4 × 33 mL). The combined organic layers dried over Na₂SO₄, filtered and partially concentrated (volume ~33 mL, 0.20 M) by rotary evaporation. To this solution was added aqueous 50% NaOH (0.343 mL, 0.520 g solution, 0.260 g NaOH, 6.50 mmol) over 1 min with rapid stirring. The suspension was stirred for 20 min at 23 °C, causing a white precipitate to form. The flask was then sonicated for 5 min and the white precipitate was collected by concentration in vacuo or by filtration through a medium porosity glass frit, rinsing with MTBE. The product was dried under vacuum at <1 mbar at 23 °C for 10 h to give the corresponding trihydroxyborate salt as a colorless, free-flowing powder. For full experimental details, ¹H NMR, and ¹³C NMR spectra see Supplementary Methods.

Synthesis of boronic acids as dioxane solutions. Sodium alkyltrihydroxyborate (1.50 mmol, 1.00 equiv.) was added to a 2-mL screw-cap vial with a stir bar. Anhydrous dioxane (1.15 mL, 1.3 M) was added and the slurry was vigorously stirred. BF₃·OEt₂ (0.185 mL, 0.213 g, 1.50 mmol, 1.00 equiv.) was added dropwise over 15 min under air. If the mixture became unstirrable, it was periodically capped and shaken by hand. After completion of the addition, the vial was capped and stirred for 20 min. The resulting fine suspension was filtered by passing through a Pasteur pipette containing 40 mg of Celite over a small cotton plug, using air pressure. The residue from the vial was washed through with additional dioxane (0.35 mL, 1.0 M theoretical concentration). The resulting homogeneous solution amounted to 1.15 mL. An aliquot of this solution (30 μL, 30 μmol theoretical) was combined with a standard solution DMSO-d₆ and 1,4-dimethoxybenzene (0.050 M, 0.60 mL, 30 μmol 1,4-dimethoxybenzene) in an NMR tube. The boronic acid was analyzed by ¹H-NMR and the concentration of boronic acid was determined. This solution was diluted to 0.91 M by adding dry dioxane (0.20 mL) and was then transferred in a capped vial into a glovebox and used directly in cross coupling reactions. For full experimental details, ¹H NMR, and ¹³C NMR spectra see Supplementary Methods.

Cross-coupling of secondary boronic acids. To a stir bar-equipped 7 mL vial were added L4 (5.3 mg, 0.010 mmol, 10 mol%), Pd₂dba₃ (4.6 mg, 0.0050 mmol, 5 mol%), aryl or vinyl halide (0.100 mmol, 1.00 equiv.), and Ag₂O (34.8 mg, 0.3 mmol, 1.5 equiv.). A dioxane solution of freshly prepared boronic acid (0.91 M, 0.220 mL, 0.200 mmol, 2.00 equiv.) was added by pipette. The vial was tightly sealed with a teflon-lined screw cap and stirred at 200 rpm at 85 °C for 24 h. Upon completion, the reaction mixture was filtered through a silica gel plug in a Pasteur pipette, rinsing with EtOAc or Et₂O. An aliquot of the crude reaction mixture was subjected to HPLC analysis to determine the b/l product ratio, comparing with an authentic sample of the linear product isomer. The crude reaction was then purified by column chromatography on silica gel, and the enantiospecificity was determined by chiral HPLC. For full experimental details, ¹H NMR, and ¹³C NMR spectra see Supplementary Methods.

Data availability

The authors declare that the data supporting the findings of this study are available within the article and its supplementary information files. The X-ray crystallographic coordinates for structures reported in this study have been deposited at the Cambridge Crystallographic Data Centre (CCDC), under deposition numbers **SI-45** 1838473, **SI-46** 1838474, **5a** 1838475 and **6i** 1894457. These data can be obtained free of charge from The Cambridge Crystallographic Data Centre via www.ccdc.cam.ac.uk/data_request/cif

Received: 22 January 2019 Accepted: 20 February 2019

Published online: 20 March 2019

References

- Blakemore, D. C. et al. Organic synthesis provides opportunities to transform drug discovery. *Nat. Chem.* **10**, 383–394 (2018).
- Choi, J. & Fu, G. C. Transition metal-catalyzed alkyl-alkyl bond formation. Another dimension in cross-coupling chemistry. *Science* **356**, eaaf7230 (2017).
- Wang, C.-Y., Derosaa, J. & Biscoe, M. R. Configurationally stable, enantioenriched organometallic nucleophiles in stereospecific Pd-catalyzed cross-coupling reactions. An alternative approach to asymmetric synthesis. *Chem. Sci.* **6**, 5105–5113 (2015).
- Cherney, A. H., Kadunce, N. T. & Reisman, S. E. Enantioselective and enantiospecific transition-metal-catalyzed cross-coupling reactions of organometallic reagents to construct C-C bonds. *Chem. Rev.* **115**, 9587–9652 (2015).
- Harris, M. R., Hanna, L. E., Greene, M. A., Moore, C. E. & Jarvo, E. R. Retention or inversion in stereospecific nickel-catalyzed cross-coupling of benzylic carbamates with arylboronic esters. Control of absolute stereochemistry with an achiral catalyst. *J. Am. Chem. Soc.* **135**, 3303–3306 (2013).
- Zhou, Q., Cobb, K. M., Tan, T. & Watson, M. P. Stereospecific cross couplings to set benzylic, all-carbon quaternary stereocenters in high enantiopurity. *J. Am. Chem. Soc.* **138**, 12057–12060 (2016).
- Schmidt, J., Choi, J., Liu, A. T., Slusarczyk, M. & Fu, G. C. A general, modular method for the catalytic asymmetric synthesis of alkylboronate esters. *Science* **354**, 1265–1269 (2016).
- Perera, D. et al. A platform for automated nanomole-scale reaction screening and micromole-scale synthesis in flow. *Science* **359**, 429–434 (2018).
- Li, J. et al. Synthesis of many different types of organic small molecules using one automated process. *Science* **347**, 1221–1226 (2015).
- Imao, D., Glasspoole, B. W., Laberge, V. S. & Crudden, C. M. Cross coupling reactions of chiral secondary organoboron esters with retention of configuration. *J. Am. Chem. Soc.* **131**, 5024–5025 (2009).
- Awano, T., Ohmura, T. & Suginome, M. Inversion or retention? Effects of acidic additives on the stereochemical course in enantiospecific Suzuki-Miyaura coupling of α -(acetyl amino)benzylboronic esters. *J. Am. Chem. Soc.* **133**, 20738–20741 (2011).
- Molander, G. A. & Wisniewski, S. R. Stereospecific cross-coupling of secondary organotrifluoroborates. Potassium 1-(benzyloxy) alkyltrifluoroborates. *J. Am. Chem. Soc.* **134**, 16856–16868 (2012).
- Sandrock, D. L., Jean-Gérard, L., Chen, C.-y., Dreher, S. D. & Molander, G. A. Stereospecific cross-coupling of secondary alkyl β -trifluoroboratoamides. *J. Am. Chem. Soc.* **132**, 17108–17110 (2010).
- Ohmura, T., Awano, T. & Suginome, M. Stereospecific Suzuki-Miyaura coupling of chiral α -(acylamino)benzylboronic esters with inversion of configuration. *J. Am. Chem. Soc.* **132**, 13191–13193 (2010).
- Lee, J. C. H., McDonald, R. & Hall, D. G. Enantioselective preparation and chemoselective cross-coupling of 1,1-diboron compounds. *Nat. Chem.* **3**, 894–899 (2011).
- Li, L., Zhao, S., Joshi-Pangu, A., Diane, M. & Biscoe, M. R. Stereospecific Pd-catalyzed cross-coupling reactions of secondary alkylboron nucleophiles and aryl chlorides. *J. Am. Chem. Soc.* **136**, 14027–14030 (2014).
- Hoang, G. L. & Takacs, J. M. Enantioselective γ -borylation of unsaturated amides and stereoretentive Suzuki-Miyaura cross-coupling. *Chem. Sci.* **8**, 4511–4516 (2017).
- Blaisdell, T. P. & Morken, J. P. Hydroxyl-directed cross-coupling. A scalable synthesis of debromohamigeran E and other targets of interest. *J. Am. Chem. Soc.* **137**, 8712–8715 (2015).
- Rygus, J. P. G. & Crudden, C. M. Enantiospecific and Iterative Suzuki-Miyaura cross-couplings. *J. Am. Chem. Soc.* **139**, 18124–18137 (2017).
- Carrow, B. P. & Hartwig, J. F. Distinguishing between pathways for transmetalation in Suzuki-Miyaura reactions. *J. Am. Chem. Soc.* **133**, 2116–2119 (2011).
- Amatore, C., Jutand, A. & Le Duc, G. Kinetic data for the transmetalation/reductive elimination in palladium-catalyzed Suzuki-Miyaura reactions. Unexpected triple role of hydroxide ions used as base. *Chem. Eur. J.* **17**, 2492–2503 (2011).
- Thomas, A. A. & Denmark, S. E. Pre-transmetalation intermediates in the Suzuki-Miyaura reaction revealed. The missing link. *Science* **352**, 329–332 (2016).
- Jover, J., Fey, N., Purdie, M., Lloyd-Jones, G. C. & Harvey, J. N. A computational study of phosphine ligand effects in Suzuki-Miyaura coupling. *J. Mol. Catal.* **324**, 39–47 (2010).
- Thomas, A. A., Wang, H., Zahrt, A. F. & Denmark, S. E. Structural, kinetic, and computational characterization of the elusive Arylpalladium(II)boronate complexes in the Suzuki-Miyaura reaction. *J. Am. Chem. Soc.* **139**, 3805–3821 (2017).
- Ye, J., Bhatt, R. K. & Falck, J. R. Stereospecific palladium/copper cocatalyzed cross-coupling of α -alkoxy- and α -aminostannanes with acyl chlorides. *J. Am. Chem. Soc.* **116**, 1–5 (1994).
- Espinat, P. & Echavarren, A. M. The mechanisms of the Stille reaction. *Angew. Chem. Int. Ed.* **43**, 4704–4734 (2004).
- Hatanaka, Y. & Hiyama, T. Stereochemistry of the cross-coupling reaction of chiral alkylsilanes with aryl triflates. A novel approach to optically active compounds. *J. Am. Chem. Soc.* **112**, 7793–7794 (1990).
- Cross, R. J. in: A.G. Sykes (Ed), *Advances in Inorganic Chemistry Academic Press*, pp. 219–292 (Elsevier, 1989).
- Johnson, L. K., Killian, C. M. & Brookhart, M. New Pd(II)- and Ni(II)-based catalysts for polymerization of ethylene and α -olefins. *J. Am. Chem. Soc.* **117**, 6414–6415 (1995).
- Allen, K. E., Campos, J., Daugulis, O. & Brookhart, M. Living polymerization of ethylene and copolymerization of ethylene/methyl acrylate using “Sandwich” diimine palladium catalysts. *ACS Catalysis* **5**, 456–464 (2014).
- Paul, F., Patt, J. & Hartwig, J. F. Palladium-catalyzed formation of carbon-nitrogen bonds. Reaction intermediates and catalyst improvements in the hetero cross-coupling of aryl halides and tin amides. *J. Am. Chem. Soc.* **116**, 5969–5970 (1994).
- Hartwig, J. F., Richards, S., Barañano, D. & Paul, F. Influences on the relative rates for C–N bond-forming reductive elimination and β -hydrogen elimination of amides. A case study on the origins of competing reduction in the palladium-catalyzed amination of aryl halides. *J. Am. Chem. Soc.* **118**, 3626–3633 (1996).
- Zou, G., Reddy, Y. K. & Falck, J. R. Ag(I)-promoted Suzuki-Miyaura cross-couplings of n -alkylboronic acids. *Tetrahedron Lett.* **42**, 7213–7215 (2001).
- Falck, J. R., Kumar, P. S., Reddy, Y. K., Zou, G. & Capdevila, J. H. Stereospecific synthesis of EET metabolites via Suzuki-Miyaura coupling. *Tetrahedron Lett.* **42**, 7211–7212 (2001).
- Stambuli, J. P., Incarvito, C. D., Bühl, M. & Hartwig, J. F. Synthesis, structure, theoretical studies, and ligand exchange reactions of monomeric, T-shaped arylpalladium(II) halide complexes with an additional, weak agostic interaction. *J. Am. Chem. Soc.* **126**, 1184–1194 (2004).
- Tolman, C. A. Steric effects of phosphorus ligands in organometallic chemistry and homogeneous catalysis. *Chem. Rev.* **77**, 313–348 (1977).
- Zhao, S. et al. Enantiodivergent Pd-catalyzed C-C bond formation enabled through ligand parameterization. *Science* **362**, 670–674 (2018).
- Li, J. & Burke, M. D. Pinene-derived iminodiacetic acid (PIDA). A powerful ligand for stereoselective synthesis and iterative cross-coupling of C(sp³) boronate building blocks. *J. Am. Chem. Soc.* **133**, 13774–13777 (2011).
- Yoon, J.-M., Lee, C.-Y., Jo, Y.-I. & Cheon, C.-H. Synthesis of optically pure 3,3'-disubstituted-1,1'-bi-6-methoxy-2-phenol (BIPOL) derivatives via diastereomeric resolution. *J. Org. Chem.* **81**, 8464–8469 (2016).
- Cambridge, A. N. et al. Aryl trihydroxyborates. Easily isolated discrete species convenient for direct application in coupling reactions. *Org. Lett.* **8**, 4071–4074 (2006).
- Jang, Y.-W. et al. Xylarinic acids A and B, new antifungal polypropionates from the fruiting body of *Xylaria polymorpha*. *J. Antibiot.* **60**, 696–699 (2007).
- Schmidt, Y., Lehr, K., Colas, L. & Breit, B. Assignment of relative configuration of desoxypropionates by 1H NMR spectroscopy. Method development, proof of principle by asymmetric total synthesis of xylarinic acid A and applications. *Chem. Eur. J.* **18**, 7071–7081 (2012).
- Labadie, J. W. & Stille, J. K. Mechanisms of the palladium-catalyzed couplings of acid chlorides with organotin reagents. *J. Am. Chem. Soc.* **105**, 6129–6137 (1983).
- Li, L., Wang, C.-Y., Huang, R. & Biscoe, M. R. Stereoretentive Pd-catalyzed Stille cross-coupling reactions of secondary alkyl azastannatranes and aryl halides. *Nat. Chem.* **5**, 607–612 (2013).

Acknowledgements

The authors gratefully acknowledge the NSF (CHE 15–66071) and the NIH (GM118185) for financial support, Andrea Palazzolo for synthesis of some phosphine-ligands, Johnson Matthey for a gift of palladium catalysts, Dr. Danielle Gray for X-ray analysis, and the School of Chemical Sciences NMR Lab at the University of Illinois for NMR services. D.J.B. is an Illini 4000 Post-doctoral Fellow of the Damon Runyon Cancer Research Foundation (DRG-2290-17) and M.T. is an Erwin Schrödinger Post-Doctoral Fellow,

Austrian Science Fund (FWF):[J3960-N34]. Scott Denmark is also gratefully acknowledged for review of this manuscript.

Author contributions

M.D.B., P.W., I.T.C. and J.W.L. conceived this project. J.W.L., I.T.C., D.J.B., M.T., P.W., J.L. and M.D.B. designed and executed the experiments. J.W.L. and M.D.B. wrote the paper.

Additional information

Supplementary Information accompanies this paper at <https://doi.org/10.1038/s41467-019-09249-z>.

Competing interests: The University of Illinois has filed patent applications on ligands and methods reported in this manuscript, and some of these have been licensed to REVOLUTION Medicines, a company for which M.D.B. is a founder. All the remaining authors declare no competing interests.

Reprints and permission information is available online at <http://npg.nature.com/reprintsandpermissions/>

Journal Peer Review Information: *Nature Communications* thanks the anonymous reviewers for their contribution to the peer review of this work.

Publisher's note: Springer Nature remains neutral with regard to jurisdictional claims in published maps and institutional affiliations.



Open Access This article is licensed under a Creative Commons Attribution 4.0 International License, which permits use, sharing, adaptation, distribution and reproduction in any medium or format, as long as you give appropriate credit to the original author(s) and the source, provide a link to the Creative Commons license, and indicate if changes were made. The images or other third party material in this article are included in the article's Creative Commons license, unless indicated otherwise in a credit line to the material. If material is not included in the article's Creative Commons license and your intended use is not permitted by statutory regulation or exceeds the permitted use, you will need to obtain permission directly from the copyright holder. To view a copy of this license, visit <http://creativecommons.org/licenses/by/4.0/>.

© The Author(s) 2019